Xe@cryptophane Complexes with C_2 Symmetry: Synthesis and Investigations by ^{129}Xe NMR of the Consequences of the Size of the Host Cavity for Xenon Encapsulation

Thierry Brotin[a] and Jean-Pierre Dutasta*[a]

Keywords: Supramolecular chemistry / Cryptophanes / Host-guest systems / NMR spectroscopy / Xenon

New cryptophanes-223 (**1**), -233 (**2**), and -224 (**3**) with C_2 symmetry, bearing different linkers connecting the two cyclotriveratrylene units were synthesized following a multistep procedure. The formation of the xenon@cryptophane complexes was investigated by ^{129}Xe NMR spectroscopy. Cryptophanes-223 (**1**) and -233 (**2**) complex xenon efficiently in 1,1,2,2-[D_2]tetrachloroethane solution with somewhat lower binding constants (K = 2810 M^{-1} and 810 M^{-1} respectively at 278 K) than that observed with cryptophane-A (K = 3900 M^{-1}). The free and bound guests were observed at room temperature under slow-exchange conditions on the ^{129}Xe NMR timescale. A linear relationship was observed between the binding constants and the internal volume of the hosts. Under the same conditions, the Xe@cryptophane-224 [Xe**3**] complex underwent a fast-exchange process on the NMR timescale. The decomplexation activation energies E_a, and the associated parameters $\Delta H^{\ddagger}$ and $\Delta S^{\ddagger}$, were determined for the Xe**1** and Xe**2** complexes from variable temperature 1D-EXSY experiments. These investigations emphasized the importance of the size of the internal cavity of the cryptophanes for guest encapsulation, and the extreme sensitivity of the ^{129}Xe chemical shift toward slight structural modifications of the atom's environment.

Introduction

Small neutral molecules are known to interact weakly with their environment, mainly through van der Waals forces. Therefore, the design of original organic receptors able to encapsulate guests such as helium or xenon atoms is still a challenging topic.[1−4] Cryptophane-A, which belongs to a well-known family of supramolecular hosts, has demonstrated its ability to encapsulate monatomic xenon efficiently with a surprisingly high binding constant, $K \approx 3900\ M^{-1}$ at 278 K.[5] The extraordinary sensitivity of the ^{129}Xe chemical shift to the atom's environment, and particularly to the confined space of the cryptophane cavity, allowed us to discriminate between cryptophane-A and its deuterated congeners.[6] This exceptional property suggests that the size of the internal cavity of cryptophane-A is well suited to encapsulate xenon, thus maximizing host−guest interactions. This was further supported by studying xenon complexation with cryptophane-E, which possesses three propylene bridges connecting the two cyclotriveratrylene units, instead of the ethylene bridges in cryptophane-A. Consequently, cryptophane-E has a larger inner cavity than cryptophane-A, and complexes monoatomic xenon poorly ($K \approx 5-10\ M^{-1}$ at 278 K in 1,1,2,2-tetrachloroethane).[7] The ^{129}Xe NMR spectrum of a mixture of xenon and cryptophane-E revealed only one broad signal located at high frequency, corresponding to free xenon in solution under fast-exchange conditions on the NMR timescale. This result shows that a slight change in the volume of the molecular cavity of the cryptophanes has a dramatic effect on the complexing properties towards xenon. Such a dependence of guest recognition on the internal volume of hosts has already been reported for other supramolecular systems and plays an important role in the encapsulation of neutral molecules inside molecular cavities.[8]

In this paper, we report the synthesis of the new cryptophanes-223 (**1**), -233 (**2**) and -224 (**3**) bearing different linkers, where -223, -233 and -224 indicate the number of methylene groups in each of the three linkers [e.g. -223 stands for two $(CH_2)_2$ and one $(CH_2)_3$ linkers]. Accordingly, cryptophane-A and -E should be labeled -222 and -333 respectively. However, we will keep the former nomenclature throughout this paper. We found that cryptophane-223 and -233, for which the sizes of the internal cavities lie between those of cryptophane-A and cryptophane-E, complex xenon efficiently in solution under slow-exchange conditions on the NMR timescale. We also determined the decomplexation activation energy and the associated parameters $\Delta H^{\ddagger}$ and $\Delta S^{\ddagger}$ of the new Xe@cryptophane complexes from a series of ^{129}Xe 1D-EXSY NMR experiments performed at several temperatures.

[a] Stéréochimie et Interactions Moléculaires, École Normale Supérieure de Lyon, UMR CNRS no. 5532,
46 Allée d'Italie, 69364 Lyon 07, France
Fax: (internat.) + 33-4/72728483
E-mail: dutasta@ens-lyon.fr

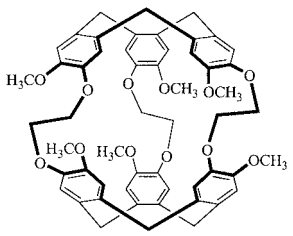
Cryptophane-A

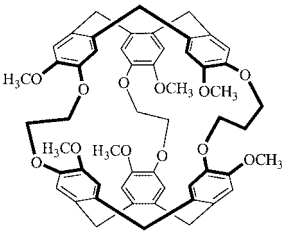
Cryptophane-223 (**1**)

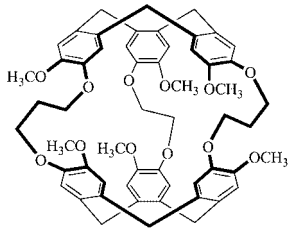
Cryptophane-233 (**2**)

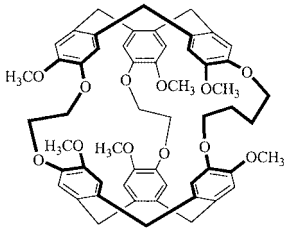
Cryptophane-224 (**3**)

Results and Discussion

Synthesis and Characterization

The synthesis of the new cryptophanes **1**−**3** was achieved by following the experimental procedure previously described for the synthesis of deuterated cryptophane-A.[9] This method requires the generation of the two cyclotriveratrylene caps at different stages of the synthesis, and usually gives rise to cryptophanes in moderate to good yields, depending on their chemical structure. The formation of the cryptophanes from their precursors was predicted from mass spectrometry experiments. Indeed, we have recently demonstrated that when cryptophanes are formed from their precursors during LSIMS experiments, they can be prepared using standard synthetic procedures.[10]

Vanillyl alcohol (**4**) was allowed to react with allyl bromide in acetone in the presence of potassium carbonate to give the protected compound **5** (Scheme 1). This is the key compound for generating cyclotriveratrylene **6** in two steps, in fairly good yields, according to a known procedure.[11] Vanillyl alcohol was also used to prepare compounds **7**−**9** bearing bromoalkyl chains with different lengths. Following the standard procedure using potassium carbonate in acetone and the appropriate dibromoalkane, they were obtained from **4** in low (25%, **7**)[12,13] to good yields (65%, **8**;[12,13] 75%, **9**). The tetrahydropyranyl ether (OTHP) functions, introduced as protecting groups in the cryptophane precursors, considerably facilitated their purification by column chromatography on silica gel and did not alter the final cyclization step. Thus, reaction of **7** and **8** with dihydropyran and pyridinium *p*-toluenesulfonate (PPTS) in a mixture of THF and dichloromethane led to compounds **10** and **11**, respectively in 80% yield. The corresponding iodinated derivatives were obtained in quantitative yield by treatment with an excess of sodium iodide in acetone to give compounds **12**−**16** (Scheme 1).[9,12,13]

The preparation of cryptophanes **1**−**3** required a slightly different strategy from that used for the cryptophanes with D_3 symmetry. In the present case we needed to introduce different substituents on the cyclotriveratrylene **6**. This could be achieved only through a stepwise synthesis introducing the different substituents successively in order to obtain the desired cryptophanes (Scheme 2). Such a strategy was successfully applied to introduce a single deuterated methyl group or two deuterated alkyl chains in a cryptophane structure.[9] Reaction of **6** with two equivalents of cesium carbonate in DMF and the appropriate iodinated compounds **12**, **13** and **14** afforded compounds **17** (30%),[9] **18** (32%) and **19** (33%) respectively. The terminal benzyl alcohol function was kept unprotected in order to facilitate

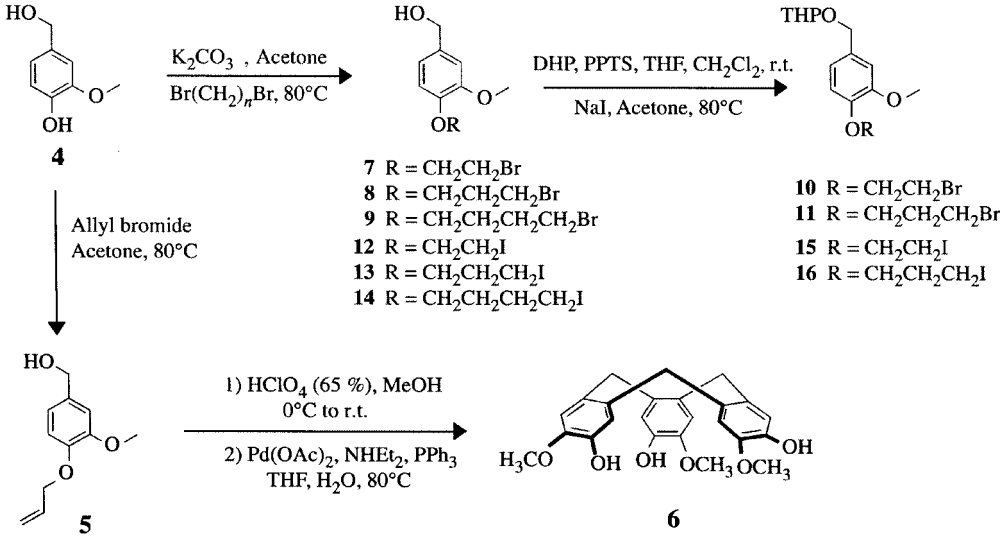

Scheme 1

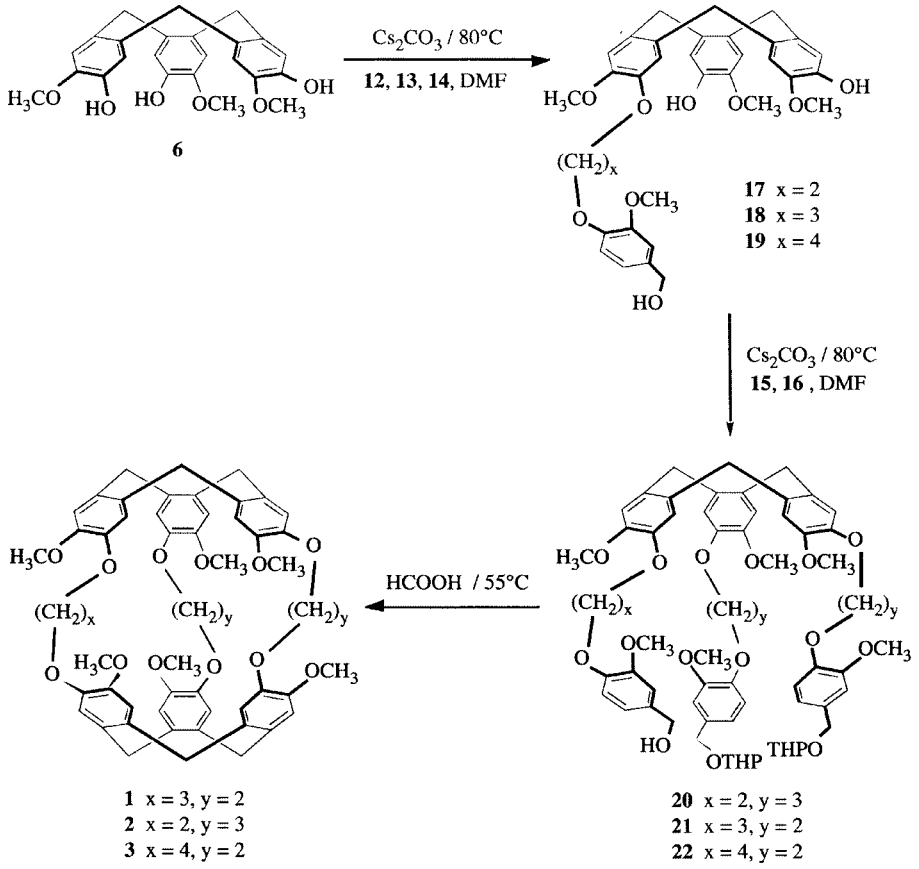

Scheme 2

the chromatographic separation of the desired material on silica gel. Side products were mainly the di- and trisubstituted derivatives, which were obtained in similar yields. Cryptophane precursors **20**−**22** were prepared from **17**−**19** by reaction with compounds **15** or **16** in good yields (72 to 79%) after column chromatography on silica gel.

The new cryptophanes **1**, **2** and **3** were then obtained from their precursors **21**, **20** and **22** respectively, by treatment in formic acid. The yields were 35−40% after purification, significantly lower than that obtained with cryptophane-A (70%) prepared under the same experimental conditions. Presumably, the dissymmetry of the precursors did not favor the cyclization step and therefore increased the formation of side-products.

The ^{1}H NMR spectra (Figure 1) recorded in chloroform, and the ^{13}C NMR spectra of compounds **1**−**3** are in good agreement with a structure with C_2 symmetry. In the ^{1}H NMR spectra of **1**−**3**, the aromatic and methyl protons give six and three signals respectively. In addition, for each compound different patterns were observed for the axial and the equatorial protons of the methylene bridges, as a consequence of the dissymmetry of the molecules.

Nevertheless, these observations are not sufficient to fully describe the structure of compounds **1**−**3**. Indeed, the strategy used to synthesize the cryptophanes can lead to the *syn* (achiral, C_s symmetry) and/or the *anti* isomers (chiral, C_2

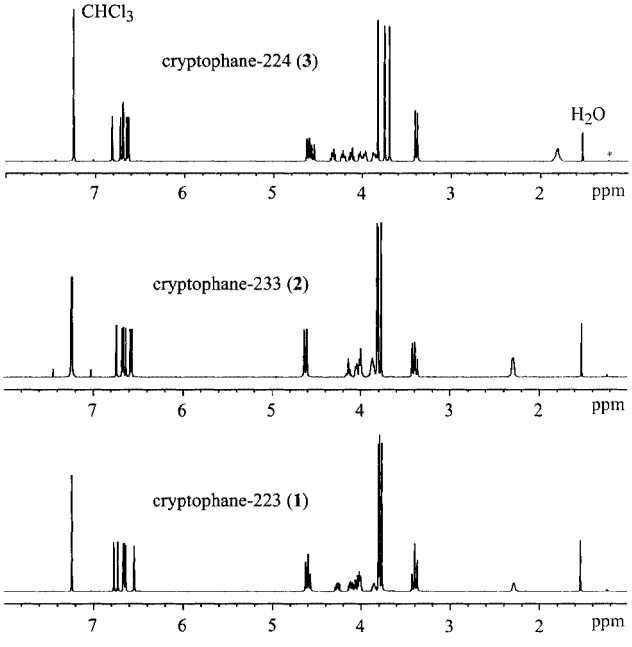

Figure 1. ^{1}H NMR spectra of cryptophanes **1**−**3** in deuterated chloroform at 293 K (* impurity from the solvent)

symmetry), undistinguishable from their ^{1}H NMR spectra. The stereochemistry of compounds **1** and **2** was determined by chiral HPLC using a Chiralpak OT$^+$ column. This technique was successfully used to discriminate the two enantiomers of the *anti* isomer of cryptophane-A and related compounds.[14,15] Both compounds **1** and **2** exhibite two close peaks of equal intensity indicating that we isolated the *anti* isomer (C_2 symmetry). HPLC analysis of **3** showed only one broad signal, presumably due to a very low resolution, which prevented the characterization of both enantiomers.[16] However, the *syn* isomers of cryptophanes bearing $O(CH_2)_2O$ linkers have never yet been observed, and we tentatively assigned the *anti* configuration to cryptophane **3**. Only an X-ray structural determination could ascertain the stereochemistry of host **3**. Unfortunately, so far we have not obtained crystals suitable for X-ray analysis.

^{129}Xe NMR Studies of the Xe@cryptophane Complexes

The ^{129}Xe NMR spectra of the Xe@cryptophane-223, -233 and -224 complexes were first studied separately at several temperatures in 1,1,2,2-[D_2]tetrachloroethane (Figure 2). At room temperature, we observed the resonance of the free and bound xenon in molecules **1** and **2** (slow-exchange conditions). Encapsulation of xenon by cryptophane-233 (**2**) seems surprising since the structure of this molecule is probably closer to the structure of cryptophane-E than that of cryptophane-A. We also noticed a large chemical-shift difference for the resonance of bound xenon encapsulated within the three cryptophanes. The difference becomes even larger upon decreasing the temperature. At 293 K the chemical shift differences between free and bound xenon in molecules **1** and **2** are δ = 164.0 and δ = 177.0 ppm, respectively (vs. δ = 156.0 ppm for cryptophane-A). At 238 K the peaks are narrower and the chemical shift differences between free and bound xenon in **1** and **2** are δ = 201.0 and δ = 211.0 ppm, respectively. The shielding environment of the benzene rings of the host molecule is not the major contributor to the large chemical shift difference observed between the free and bound xenon. As reported by Bartik et al., intermolecular interactions, and particularly van der Waals interactions, are by far the most important effect because of the large polarizable electron cloud of the xenon atom.[5] However, because the environment of the bound guest within the three cryptophanes is very similar, an additional factor has to be considered to explain the different chemical shifts observed for each complex.

It is well-known that the xenon chemical shift is highly sensitive to slight variations of the volume of the molecular cavity, which defines the close surroundings of the xenon atom.[17] The differences observed for the resonance of the xenon encapsulated within the cavity of each cryptophane host probably arise from a change of the cavity size. Bound xenon should be less confined in **2** than in cryptophane-A, explaining the low frequency shift observed with Xe**2**. It is obvious that a change in the length of the $O(CH_2)_nO$ linkers will modify the size of the windows of the cryptophanes and consequently should affect the dynamics of the complexation process. This point will be discussed later. The ^{129}Xe NMR spectrum of a solution containing xenon and cryptophane-224 (**3**) was recorded at 233 K (Figure 2, c). The spectrum showed only one broad signal at δ = 245 ppm, the value for free xenon. The absence of a resonance for bound xenon suggested that we were under fast-exchange conditions on the NMR timescale and the

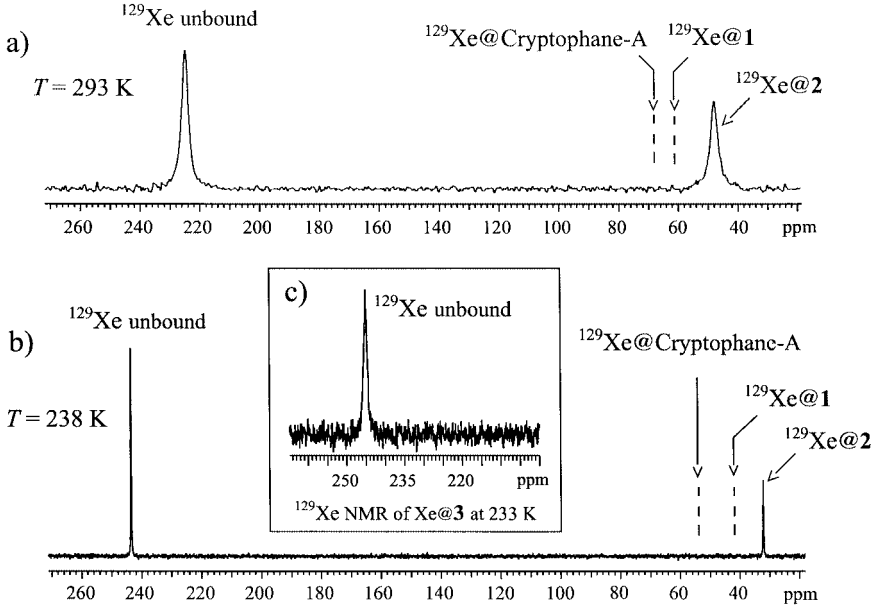

Figure 2. ^{129}Xenon NMR spectrum of the of Xe@cryptophane-233 complexes [Xe**2**] in 1,1,2,2-[D_2]tetrachloroethane; the ^{129}Xe NMR signals of xenon encapsulated into cryptophane-A and cryptophane-223 (**1**) are also shown for comparison; a) 293 K, b) 238 K; c) ^{129}Xe NMR spectrum of a solution containing cryptophane-224 (**3**) in 1,1,2,2-[D_2]tetrachloroethane solution at 233 K (only the resonance of the unbound xenon is observed under fast-exchange conditions on the NMR timescale)

Table 1. Volume V (Å^3) of the internal cavities of cryptophanes-A, -E and **1**−**3**

	Cryptophane-A	Cryptophane-223 (**1**)	Cryptophane-233 (**2**)	Cryptophane-224 (**3**)	Cryptophane-E
V (Å^3)	95.0	102.1	117.2	109.9	120.9

broadening observed for the free xenon line was due to xenon going into **3** with a rather short residence time. To confirm these observations the sizes of the internal cavities of the new cryptophanes **1**−**3** were calculated by molecular modeling.[18] The results reported in Table 1, represent the volume of the internal cavity of the minimized structure of the cryptophanes in the gas phase. As expected, the dimensions of the internal cavity increase on going from cryptophane-A to cryptophane-E except for cryptophane-224 (**3**), where they are between those of cryptophane-223 (**1**) and cryptophane-233 (**2**).

This result is surprising since we have observed that in solution xenon binding to cryptophane-224 (**3**) is not as efficient as to cryptophane-233 (**2**). The conclusion is probably that the $O(CH_2)_4O$ linker exists in several conformations close in energy, which can significantly change the size of the internal cavity. The increased flexibility due to the $O(CH_2)_4O$ linker prevents the formation of a stable Xe**3** complex. Additionally, with the larger cryptophane **3**, the solvent may compete with the guest. However, this is difficult to verify experimentally owing to the lack of available noncompeting solvents.

Binding constants of the new Xe**1** and Xe**2** complexes were measured by competition experiments. A solution containing equimolar amounts of cryptophane-A and **1** was prepared in 1,1,2,2-tetrachloroethane in the presence of an excess of xenon. The ^{129}Xe NMR spectrum was then recorded at 278 K (Figure 3, a). Similarly, a second sample was prepared by mixing equimolar amounts of cryptophanes **1** and **2** (Figure 3, b).

As expected, the two samples showed the presence of three signals, for the free xenon and the two corresponding Xe@cryptophane complexes. In the first sample, the intensity of the signal for Xe**1** is significantly lower than that for Xe@cryptophane-A, suggesting a lower binding constant for **1** than for cryptophane-A. Similarly, in the second sample, a significant decrease of the signal of Xe**2** is observed with respect to Xe**1**. This is in good agreement with an increase of the volume of the internal cavity of hosts **1** and **2** with respect to cryptophane-A. The association constants for the new complexes Xe**1** (K = 2810 м$^{-1}$) and Xe**2** (K = 810 м$^{-1}$) were obtained from the peak intensities of the corresponding xenon signals and the known binding constant for Xe@cryptophane-A (K = 3900 м$^{-1}$).

These results show that a slight modification in the structure of the hosts (volume of the internal cavity) significantly affects their binding properties. Additionally, we observed a linear relationship between the measured binding constants and the volume of the molecular cavity (Figure 4). This interesting feature suggests the possibility of predicting the complexing behavior toward xenon of cryptophanes (or, probably, any other molecules accommodating xenon). This may have important consequences, especially for designing new efficient hosts for practical applications such as biosensors, a concept that has recently been described using hyperpolarized xenon.[19]

Variable-Temperature ^{129}Xe 1D-EXSY NMR Experiments

The slow-exchange conditions observed for the complexes Xe**1** and Xe**2** allowed us to study the exchange dy-

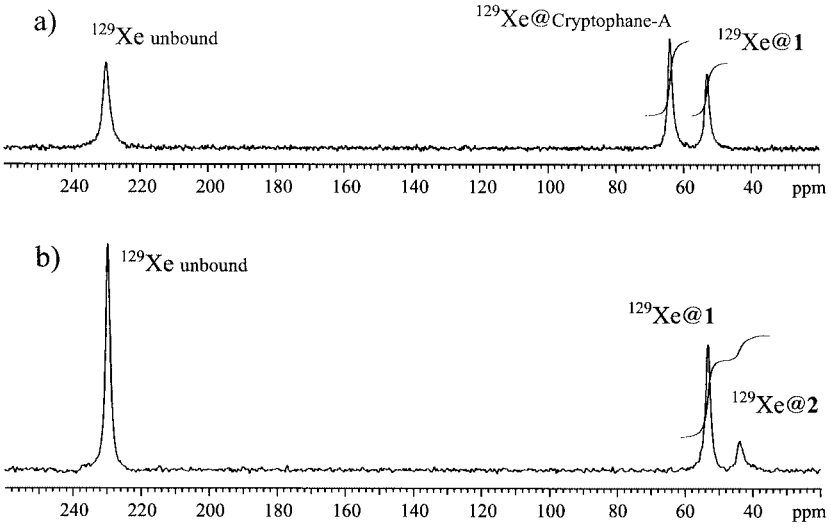

Figure 3. ^{129}Xenon NMR spectra recorded at 278 K in 1,1,2,2-tetrachloroethane of a solution containing an equimolar amount of a) cryptophane-**A** and cryptophane-223 (**1**); b) cryptophane-223 (**1**) and cryptophane-233 (**2**)

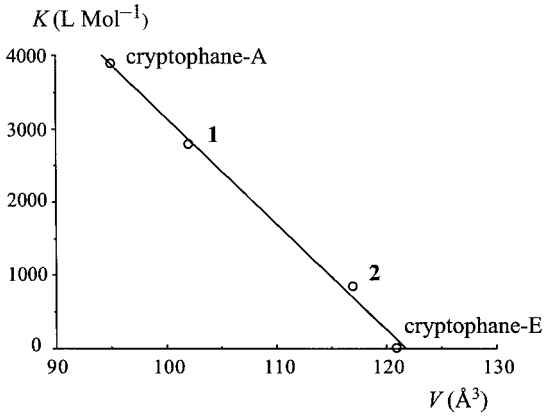

Figure 4. Plot of the measured binding constant K (M^{-1}) of cryptophanes-A, -E, **1**, and **2** as a function of the volume of the internal cavity ($r^2 = 0.996$)

namics in solution between the bound and free xenon sites.[20] The decomplexation activation energy E_a and the associated activation parameters $\Delta H^{\ddagger}$ and $\Delta S^{\ddagger}$ can be calculated from the rate constants determined at several temperatures. We successfully applied this to cryptophane-A and one of its deuterated congeners by using ^{129}Xe 1D-EXSY NMR spectroscopy.[9] We preferred the ^{129}Xe 1D-EXSY technique to 2D-EXSY for several reasons. In particular, the low number of exchanging sites, the better precision in the determination of the rate constants and the substantial decrease in the instrument time compared to 2D-EXSY, make 1D-EXSY experiments very useful for measuring the decomplexation activation energy.

We used two different methods to measure the activation parameters of the new complexes. In a first approach, we determined the activation parameters from a solution containing equimolar amounts of cryptophane-A and **1**. This method has the advantage of estimating the activation parameters of the new cryptophane with cryptophane-A as an internal standard, since its activation parameters are known. In addition it gives a good indication of the precision of our results. On the other hand, it complicates the fitting procedure since more variables are needed to fit the experimental data. We could not use a sample containing equimolar amounts of **1** and **2** to obtain accurate rate constants for **2**. The large difference of the intensities observed between the two bound states would have led to inaccurate data because of the low signal-to-noise ratio. Thus, in a second approach, we studied cryptophanes **1** and **2** separately.

The first method was thus only applied to molecule **1** (Experiment 1). A sample containing an equimolar amount of **1** and cryptophane-A in the presence of an excess of xenon was prepared and sealed under vacuum. The magnetization of the three sites (free xenon and two bound states) obeys the modified Bloch equations. The amplitude of each resonance as a function of the mixing time is given by the following matrix equation [Equation (1)], where I^i_0 is the initial magnetization of the nucleus at $\tau_m = 0$, and I^i_{eq} is the magnetization at this site for infinite relaxation time.

$$I^i(\tau_{mix}) = exp(\mathbf{L}\tau)\left(I^i_0 - I^i_{eq}\right) + I^i_{eq} \quad (1)$$

The matrix **L** is a function of the rate constants k_{ij} and the longitudinal relaxation time T_{ij} of each site for a given kinetic model. We have previously clearly demonstrated from 2D-EXSY and 1D-EXSY NMR experiments that xenon exchange between cryptophanes takes place exclusively by xenon atoms travelling through solution and that the second process involving xenon exchange by direct collision between the hosts can be neglected under our experimental conditions. Thus, we propose the following pseudo-first-order kinetic model (Scheme 3).

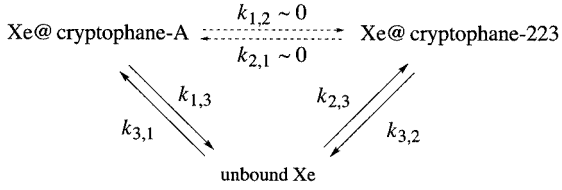

Scheme 3. Pseudo-first-order kinetic model used to describe the 1D-EXSY experiments for a sample containing an equimolar amount of cryptophane-A and cryptophane-223 (**1**) in the presence of an excess of xenon.

With this model we can describe the exchange dynamics of xenon between cryptophanes as two independent systems involving free xenon and cryptophane-A or free xenon and host **1**, respectively. Moreover, we have also clearly shown that the longitudinal relaxation time T_1, which is the same for all sites, is several orders of magnitude greater than the rate constants and can be neglected in the matrix **L**. The **L** matrix can therefore be simplified to the form given in Equation (2).[21]

$$\mathbf{L} = \begin{pmatrix} -k_{1,3} & \approx 0 & k_{3,1} \\ \approx 0 & -k_{2,3} & k_{3,2} \\ k_{1,3} & k_{2,3} & -(k_{3,1} + k_{3,2}) \end{pmatrix} \quad (2)$$

The equilibrium equation also implies $k_{1,3}/k_{3,1} = M^0_1/M^0_3$ and $k_{3,2}/k_{2,3} = M^0_2/M^0_3$ where M^0_1, M^0_2 and M^0_3 are respectively the initial magnetization ($\tau_m = 0$) of xenon bound to cryptophane-A, xenon bound to cryptophane-223 and free xenon in solution. For better precision we measured M^0_1, M^0_2 and M^0_3 by integrating the corresponding signals in the 1D ^{129}Xe NMR spectrum at a given temperature. We obtained the whole set of rate constants by irradiating independently the resonance corresponding to the free xenon in solution and the two resonances corresponding to the encapsulated xenon in both cryptophanes. This does not present any difficulties since the two signals are located very far from each other ($\delta = 190$ ppm) and a wide pulse, in the frequency domain, can be applied. However, our system cannot be studied over a large range of temperatures. Above 248 K the exchange proceeded too rapidly, and the signal-to-noise ratio decreased significantly. At too low a temper-

ature cryptophanes might precipitate or the solvent crystallize. Temperatures ranging from 248 K to 228 K were found to be suitable for these experiments using 1,1,2,2-[D_2]tetrachloroethane as solvent. We made sure that even at 228 K the solvent did not crystallize and no precipitate was observed.

Figure 5 shows the redistribution of the magnetization at 238 K as a function of the mixing time when both free and bound xenon atoms have been selectively irradiated. It took about 6.5 h to obtain rate constants at a given temperature using 32 scans for each acquisition for the 12 mixing time values. The intensities of each resonance were then measured and the rate constants for decomplexation were determined by fitting the experimental data as a function of the mixing time τ_m (Figure 6).

Rate constants decrease by a factor of five when the temperature varies from 248 K to 228 K (Table 2). The corresponding activation energies were obtained from the Arrhenius

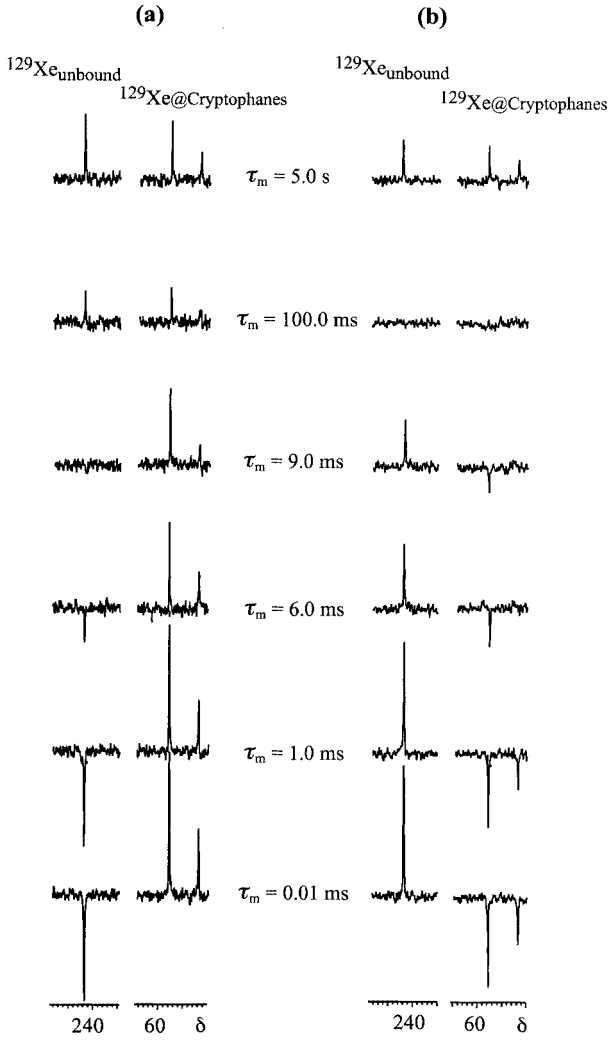

Figure 5. Evolution of the magnetization of the three sites as a function of the mixing time at 238 K (1D-EXSY): a) after selective excitation of the peak corresponding to free xenon; b) after selective excitation of the two peaks corresponding to the Xe@cryptophane complexes

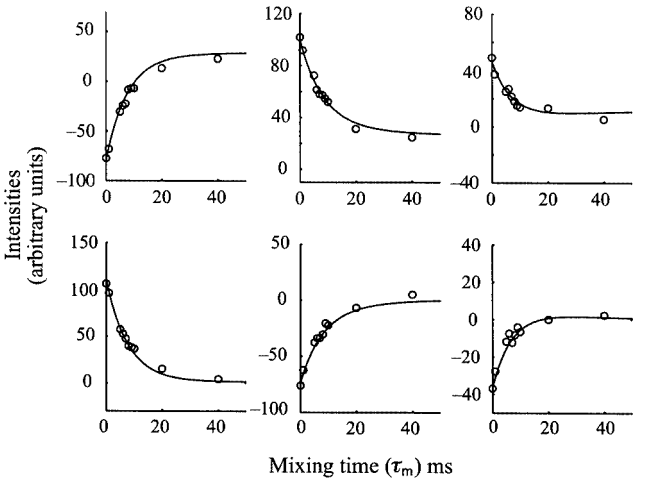

Figure 6. Evolution of the magnetization as a function of the mixing time after selective irradiation of free and encapsulated xenon; each panel represents a particular site and its evolution with τ_m (only mixing times ranging from 0 to 40 ms are shown); experimental data are represented by dots and the solid lines represent the best fit of the data

plot, ln$k$ vs. $1/T$, to give E_a = 35.5 kJ mol^{-1} and E_a = 33.1 kJ mol^{-1} for cryptophane-A and cryptophane-223, respectively (Figure 7, Table 4). The value obtained for cryptophane-A is close to that previously reported, E_a = 37.5 kJ mol^{-1}.[9] A lower value of E_a was found for cryptophane-223, consistent with an increase of the size of the cavity, which causes a decrease in the host−guest interactions. However, it should be noticed that the fit of the experimental data required a set of 14 independent parameters (nine for the initial magnetizations, three for the magnetization at equilibrium and two for rate constants). Although the use of a sample containing two cryptophanes has some advantages, it also makes the treatment of the data more complicated.

Table 2. Rate constants for decomplexation of Xe@cryptophane-A ($k_{1,3}$, M_3^0/M_1^0 = 1.1) and Xe**1** ($k_{2,3}$, M_3^0/M_2^0 = 1.8) obtained from variable temperature ^{129}Xe 1D-EXSY experiments in 1,1,2,2-[D_2]tetrachloroethane (Experiment 1)

T (K)	248	243	238	233	228
$k_{1,3}$ (s^{-1})	97.0 ± 5	66.0 ± 3	44.0 ± 3	29.5 ± 2	21.6 ± 2
$k_{2,3}$ (s^{-1})	104.9 ± 10	70.7 ± 5	51.6 ±5	35.8 ± 2	24.9 ± 2

In a second experiment (Experiment 2), a solution containing exclusively host **1** and an excess of xenon was used. 1D-EXSY experiments were then performed at different temperatures ranging from 238 K to 225 K. Similar experiments were run with a sample containing host **2** and an excess of xenon. Typical fits of the experimental data obtained with **1** at 233 K are shown in Figure 8. In this case, the fit of the experimental data requires only seven independent parameters (four for the initial magnetization, two for the magnetization at equilibrium and one for the rate

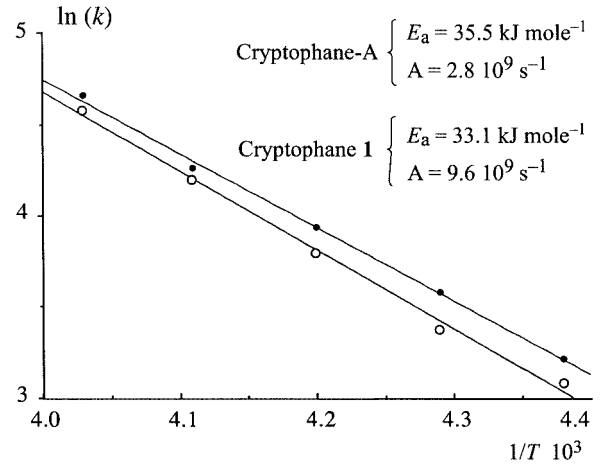

Figure 7. Arrhenius plot of $\ln(k_{1,3})$ and $\ln(k_{2,3})$ vs. $1/T$; values of $k_{1,3}$ and $k_{2,3}$ obtained from ^{129}Xe 1D-EXSY experiments at different temperatures ranging from 248 K to 228 K for cryptophane-A (o) and **1** (●)

constant) since only two exchanging sites are present in solution and the fitting curves are now represented by four panels.

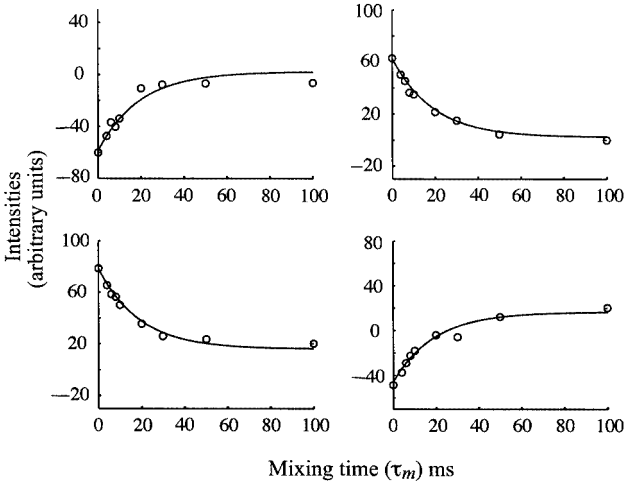

Figure 8. Evolution of the magnetizations as a function of mixing time, after selective irradiation of one of the two sites of a solution containing cryptophane-223 (**1**) and an excess of xenon at 233 K; each panel represents a particular site and its evolution with τ_m (only mixing times ranging from 10 μs to 100 ms are shown); experimental data are represented by dots and the solid lines represent the best fit of the data

The rate constants for decomplexation obtained for cryptophanes **1** and **2** at several temperatures are reported in Table 3. The decomplexation activation energies were obtained from the Arrhenius plots (Figure 9). The new value E_a = 35.1 kJ mol^{-1} for Xe**1** is close to that previously calculated in Experiment 1 (Table 4), suggesting that the mixing of two cryptophanes in the same sample has no consequences for the result, even though we believe that Experiment 2 gives more accurate data. The value for the decomplexation activation energy E_a = 34.8 kJ mol^{-1} for Xe**2** is very close to that obtained for Xe**1**.

Table 3. Rate constants for decomplexation of Xe**1** ($c \approx 0.06$ M, [^{129}Xe]/[^{129}Xe**1**] ≈ 1), and Xe **2** ($c \approx 0.06$ M, [^{129}Xe]/[^{129}Xe**2**] ≈ 1), obtained from ^{129}Xe 1D-EXSY experiments at several temperatures in 1,1,2,2-[D_2]tetrachloroethane (Experiment 2).

T (K)	243	238	233	228	225
k (s^{-1}) **1**	64.7 ± 5	39.1 ± 2	26.9 ± 2	18.5 ± 1	16.5 ± 2
k (s^{-1}) **2**	69.8 ± 6	48.9 ± 2	33.1 ± 2	21.7 ± 2	18.6 ± 1

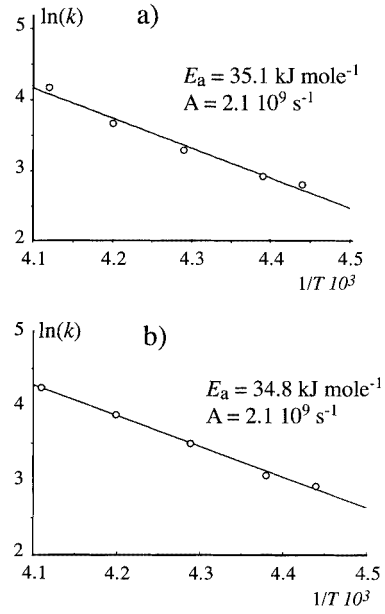

Figure 9. Arrhenius plot of ln$k$ vs. $1/T$ obtained from ^{129}Xe 1D-EXSY experiments performed at different temperatures in 1,1,2,2-[D_2]tetrachloroethane (k stands for the decomplexation rate constant); a) **1** (238 to 225 K), b) **2** (243 to 225 K)

The decomplexation activation enthalpy $\Delta H^{\ddagger}$ and entropy $\Delta S^{\ddagger}$ for cryptophane-A and compounds **1** and **2** were then obtained by plotting $\ln(k/T)$ vs. $1/T$ according to the Eyring equation [Equation (3)], where T is the absolute temperature and R is the gas constant (Table 4).

$$\ln(k/T) = 23.76 - (\Delta H^{\ddagger}/R)1/T + (\Delta S^{\ddagger}/R) \quad (3)$$

Large negative $\Delta S^{\ddagger}$ values (≈ -72 J mol^{-1} K^{-1}) were found for the new cryptophanes. As already reported for cryptophane-A this suggests that the activated Xe**1** and Xe**2** complexes are conformationally more strained than the complexes in their ground states. The values of the Gibbs activation energy, $\Delta G^{\ddagger} \approx 50$ kJ mol^{-1} at 238 K, are similar for all cryptophanes, within the limit of experimental error. The interpretation of these results is not straightforward, as molecules **1** and **2** do not have the same symmetry as cryptophane-A. The introduction of two linkers with different length decreases the symmetry of the new cryptophanes **1** and **2** (C_2 symmetry instead of D_3 symmetry for cryptophane-A), and therefore creates two portals with different

Table 4. Calculated decomplexation activation energy for cryptophane-A, **1** and **2** obtained from the Arrhenius plot ln(k) vs. 1/T; the decomplexation activation enthalpy $\Delta H^{\ddagger}$ and entropy $\Delta S^{\ddagger}$ have been calculated from an Eyring plot ln(k/T) vs. 1/T; the Gibbs activation energy of decomplexation at T = 238 K is also given

	E_a (kJ/mol)	$\Delta H^{\ddagger}$ (kJ/mol)	$\Delta S^{\ddagger}$ (J/mol K)	$\Delta G^{\ddagger}$ (kJ/mol)
Cryptophane-A[a]	37.5 ± 2.0	35.5 ± 2.0	−60.0 ± 5	49.8 ± 2.0
Cryptophane-A (Exp. 1)	35.5 ± 2.0 (r^2 = 0.993)	33.6 ± 2.0 (r^2 = 0.993)	−70.5 ± 10.0	50.4 ± 2.0
Cryptophane **1** (Exp. 1)	33.1 ± 3.0 (r^2 = 0.999)	31.3 ± 3.0 (r^2 = 0.999)	−79.0 ± 10.0	50.0 ± 2.0
Cryptophane **1** (Exp. 2)	35.1 ± 2.0 (r^2 = 0.980)	33.2 ± 2.0 (r^2 = 0.978)	−72.8 ± 10.0	50.5 ± 2.0
Cryptophane **2** (Exp. 2)	34.8 ± 2.0 (r^2 = 0.998)	32.8 ± 2.0 (r^2 = 0.998)	−71.7 ± 10.0	49.9 ± 2.0

[a] From ref.[9]

sizes. This may therefore complicate the interpretation of the experimental data since xenon may now use either of two different windows to leave molecules **1** and **2**.

Slight structural modifications, such as the addition of one or two methylene groups in the linkers, induce a substantial change of the ^{129}Xe chemical shift, and have important consequences on the stability of the Xe@cryptophane complex. However, this structural change seems to have only a small effect on the activation energies E_a. Additional support from molecular modeling would be helpful in exploring the possible ways in which the xenon guest may be extruded from the cryptophane cavity, and may give new insights leading to better interpretation of these findings.

Conclusion

We have prepared the new cryptophanes **1**−**3** with C_2 symmetry where the two cyclotriveratrylene units are connected with different alkyl chains. These compounds have been isolated as the chiral *anti* isomer, in moderate yields. The synthetic route follows a stepwise sequence of reactions, which proved to be very useful for preparing new selectively protected cryptophanes, key compounds for the elaboration of large supramolecular structures.[22] We have demonstrated that molecules **1** and **2** efficiently complex xenon in organic solution, with binding constants slightly lower than that measured with cryptophane-A, according to the increased size of the molecular cavities. Under the same experimental conditions, the affinity of xenon for **3** is considerably less than for **1** and **2**. No signal was detected for encapsulated xenon, suggesting fast-exchange conditions on the NMR timescale. In addition, a linear relationship was observed between the measured binding constant K and the volume of the inner cavity of the cryptophanes.

Measurement of the decomplexation activation energy and the associated $\Delta H^{\ddagger}$ and $\Delta S^{\ddagger}$ parameters from 1D-EXSY experiments gave values in good agreement with those previously reported for cryptophane-A. Once more, the high sensitivity of the ^{129}Xe chemical shift proved to be a powerful tool for discriminating between the slightly modified environments provided by aromatic cavities. C_2-Symmetrical cryptophanes are thus good models for investigating complexation dynamics and for correlating the physical properties of the encapsulated xenon with its environment. Efforts to design new cryptophane hosts with modified structures are currently underway, with particular application to the design of biosensors for magnetic resonance imaging.[19]

Experimental Section

General Remarks: 1,2-dibromoethane, 1,3-dibromopropane, 1,4-dibromobutane, allyl bromide and pyridinium *p*-toluenesulfonate (PPTS) were purchased from Acros Organics, and were used without further purification. Cesium carbonate and potassium carbonate were dried under vacuum before use. Solvents were distilled prior to use (DMF from calcium hydride under reduced pressure, acetone and CH_2Cl_2 from calcium chloride, THF from benzophenone ketyl ether). Column chromatographic separations were carried out over Merck silica gel 60 (0.040−0.063 mm). Analytical thin layer chromatography (TLC) was performed on MERCK silica-gel TLC plates F-254. Melting points were measured on a Perkin−Elmer DSC7 microcalorimeter. Unprotected **7**, **8**, **12** and **13**,[12,13] and protected **10** and **15**,[9] halogenated vanillyl alcohol derivatives, and monosubstituted cyclotriveratrylene **17**,[9] were synthesized using literature procedures reported by our group.

NMR Measurements: ^{129}Xe NMR experiments were carried out at 138.4 MHz on a Varian Unity$^+$ spectrometer using a 10-mm double resonance probe. The ^{129}Xe chemical shift is expressed in ppm with respect to xenon gas extrapolated to zero pressure. For competition experiments equimolar amounts of cryptophane-A (110 mg) and cryptophane-223 (**1**) (112 mg) were dissolved in 1,1,2,2-[D_2]tetrachloroethane. The solvent was evaporated under reduced pressure to remove any bound substrate (mostly $CHCl_3$). 1,1,2,2-[D_2]Tetrachloroethane (3.5 mL) was then added and the solution was poured into a 10 mm NMR tube ($c \approx 0.035$ M for each cryptophane). Xenon gas (^{129}Xe natural abundance 26.4%) was then bubbled through the solution. The same method was applied to prepare the NMR tube containing equimolar amounts of cryptophane-223 (**1**) (150 mg) and cryptophane-233 (**2**) (150 mg) in 1,1,2,2-[D_2]tetrachloroethane (3.7 mL, $c \approx 0.045$ M for each cryptophane), and the sample containing compound **3** (150 mg) in 1,1,2,2-[D_2]tetrachloroethane (3.5 mL, $c \approx 0.046$ M). ^{1}H and ^{13}C NMR spectra were run on a Varian Unity$^+$ 500 spectrometer (s:

singlet, d: doublet, t: triplet, q: quadruplet, quint: quintuplet, m: multiplet). The bridging methylene carbon of the cyclotriveratrylene moieties were labeled $C_{a,e}$, and the corresponding protons were labeled H_a (axial) and H_e (equatorial).

Complexation Dynamics as a Function of Temperature: The NMR sample containing equimolar amounts of cryptophane-A (110 mg) and cryptophane-223 (112 mg) was prepared as described above. It was then frozen in liquid nitrogen and sealed under vacuum ($c \approx 0.035$ M for each cryptophane). For ^{129}Xe 1D-EXSY NMR experiments, the sample was cooled to 248 K and kept at this temperature for about 2 h before starting experiments. The mixing times ranged from 0.01 ms to 5 s (10 or 12 values of τ_m were used for each temperature). A Gaussian pulse with duration of 139 μs was used for the 180° selective pulse. A relaxation delay of 30 s was used for each increment. Each spectrum was recorded with 32 scans for a given mixing time. The duration of the 90° pulse was 25 μs. This required about 6.5 h to complete an experiment. After each change of temperature the sample was left for 30 min before starting another experiment. In order to follow the evolution of rate constants with temperature and thus to obtain a better fit, a different set of mixing times was chosen for each temperature. Prior to the Fourier transform an exponential apodization (lb = 20) was applied. The intensity of each peak was then measured for a given vertical scale value, which was kept the same for all experiments. The NMR samples containing only molecule **1** (200 mg, $c \approx 0.06$ M) or molecule **2** (200 mg, $c \approx 0.06$ M) in 1,1,2,2-[D_2]tetrachloroethane (3.5 mL) and in the presence of an excess of xenon were prepared as described above. A Gaussian pulse with duration of 278 μs was used for the 180° selective pulse. All other parameters were the same as those described above.

(4-Bromobutoxy-3-methoxyphenyl)methanol (9): 1,4-Dibromobutane (12.63 g, 58.3 mmol) was added under argon to a stirred solution of **4** (3.0 g, 19.5 mmol), potassium carbonate (2.7 g, 19.5 mmol) in freshly distilled acetone (50 mL). The mixture was refluxed overnight under an argon atmosphere. The solvent was removed under reduced pressure and the residue was extracted with ethyl acetate. The combined organic layers were washed three times with brine, dried over Na_2SO_4 and the solvent was evaporated to leave a residue. Column chromatography (silica gel, eluent: EtOAc/pentane, 70:30) yielded **9** as a white solid (4.2 g, 75%), m.p. 58 °C. ^1H NMR (500 MHz, $CDCl_3$, 20 °C): δ = 6.91−6.81 (m, 3 H, Ar), 4.59 (s, 2 H, C*H*$_2$OH), 4.02 (t, ^3J = 6.0 Hz, 2 H, CH_2), 3.85 (s, 3 H, OCH_3), 3.48 (t, ^3J = 6.0 Hz, 2 H, CH_2Br), 2.04 (quint, ^3J = 7.0 Hz, 2 H, CH_2), 1.98 (quint, ^3J = 7.0 Hz, 2 H, CH_2), 1.64 (s, 1 H, OH) ppm. ^{13}C NMR (125.67 MHz, $CDCl_3$, 20 °C): δ = 149.44, 147.66, 133.87, 119.27, 112.96, 110.78, 68.00, 65.08, 55.80 (1 C, O*C*H$_3$), 33.48, 29.34, 27.73. $C_{12}H_{17}BrO_3$ (289.17): calcd. C 49.84, H 5.93; found C 49.79, H 5.93.

(4-Iodobutoxy-3-methoxyphenyl)methanol (14): Sodium iodide (7.8 g, 54 mmol) was added in one portion to a stirred solution of **9** (3.0 g, 10.3 mmol) in dry acetone (60 mL). The solution was stirred overnight under an argon atmosphere. After cooling, the solvent was removed to leave a residue which was extracted with ethyl acetate. The combined organic layers were washed three times with brine and dried over Na_2SO_4. Chromatography on silica gel (EtOAc/pentane, 70:30) yielded **14** as a white solid (3.3 g, 95%), m.p. 66 °C. ^1H NMR (500 MHz, $CDCl_3$, 20 °C): δ = 6.91−6.81 (m, 3 H, Ar), 4.60 (d, ^3J = 5.5 Hz, 2 H, C*H*$_2$OH), 4.02 (t, ^3J = 6.5 Hz, 2 H, OCH_2), 3.85 (s, 3 H, OCH_3), 3.25 (t, ^3J = 6.5 Hz, 2 H, CH_2I), 2.02 (quint, ^3J = 7.0 Hz, 2 H, CH_2), 1.92 (quint, ^3J = 7.0 Hz, 2 H, CH_2), 1.58 (t, ^3J = 6.5 Hz, 1 H, OH) ppm. ^{13}C NMR (125.67 MHz, $CDCl_3$, 20 °C): δ = 149.46, 147.68, 133.86, 119.28, 112.98, 110.79, 67.82, 65.11, 55.82 (1 C, O*C*H$_3$), 30.06, 29.99, 6.49 (1 C, *C*H$_2$I) ppm. $C_{12}H_{17}IO_3$ (336.17): calcd. C 42.88, H 5.10; found C 42.70, H 5.03.

2-[4-(3-Bromopropoxy)-3-methoxybenzyloxy]tetrahydropyran (11): A solution of PPTS (0.55 g, 2.18 mmol) in CH_2Cl_2 (10 mL) was added in one portion to a mixture of **8** (6.0 g, 21.8 mmol) and dihydropyran (2.65 g, 31.5 mmol) in THF (70 mL). The solution was stirred overnight at room temperature under an argon atmosphere. The solvent was removed to leave a residue which was extracted with diethyl ether. The combined organic layers were washed twice with brine, dried over Na_2SO_4 and the solvents evaporated to leave an oily residue. Chromatography on silica gel (diethyl ether/pentane, 50:50) yielded compound **11** (7.0 g, 89%) as a white solid, m.p. 37 °C. ^1H NMR (500 MHz, $CDCl_3$, 20 °C): δ = 6.90−6.85 (m, 3 H, Ar), 4.70 (d, ^2J = 11.5 Hz, 1 H), 4.67 (m, 1 H), 4.42 (d, ^2J = 11.5 Hz, 1 H), 4.13 (t, ^3J = 6.0 Hz, 2 H, OCH_2), 3.91 (m, 1 H), 3.85 (s, 3 H, OCH_3), 3.61 (t, ^3J = 6.0 Hz, 2 H, CH_2Br), 3.53 (m, 1 H), 2.34 (quint, ^3J = 6.0 Hz, 2 H, CH_2), 1.90−1.50 (m, 6 H, THP) ppm. ^{13}C NMR (125.67 MHz, $CDCl_3$, 20 °C): δ = 149.42, 147.53, 131.31, 120.46, 113.32, 111.77, 97.47, 68.64, 66.64, 62.19, 55.80 (1 C, O*C*H$_3$), 32.23, 30.50, 30.10, 25.35, 19.39 ppm. $C_{16}H_{23}BrO_4$ (359.26): calcd. C 53.49, H 6.45; found C 53.40, H 6.71.

2-[4-(3-Iodopropoxy)-3-methoxybenzyloxy]tetrahydropyran (16): Sodium iodide (12.5 g, 83.5 mmol) was added in one portion to a stirred solution of **11** (6.0 g, 16.7 mmol) in dry acetone. The solution was refluxed overnight under an argon atmosphere. After cooling to room temperature, the solvent was removed by rotary evaporation to leave a residue which was extracted with diethyl ether. The combined organic layers were washed with brine, dried over Na_2SO_4 and the solvents evaporated to leave a residue. Chromatography on silica gel (diethyl ether/pentane, 50:50) yielded **16** (6.44 g, 95%) as a white solid, m.p. 50 °C. ^1H NMR (500 MHz, $CDCl_3$, 20 °C): δ = 6.90−6.85 (m, 3 H, Ar), 4.70 (d, ^2J = 11.5 Hz, 1 H), 4.67 (m, 1 H), 4.42 (d, ^2J = 11.5 Hz, 1 H), 4.06 (t, ^3J = 6.0 Hz, 2 H, OCH_2), 3.91 (m, 1 H), 3.85 (s, 3 H, OCH_3), 3.53 (m, 1 H), 3.37 (t, ^3J = 6.0 Hz, 2 H, CH_2I), 2.29 (quint, ^3J = 6.5 Hz, 2 H, CH_2), 1.90−1.50 (m, 6 H, THP) ppm. ^{13}C NMR (125.67 MHz, $CDCl_3$, 20 °C): δ = 149.43, 147.51, 131.32, 120.46, 113.38, 111.79, 97.46, 68.59, 68.45, 62.19, 55.82 (1 C, O*C*H$_3$), 32.85, 30.50, 25.36, 19.39, 2.63 (1 C, *C*H$_2$I) ppm. $C_{16}H_{23}IO_4$ (406.26): calcd. C 47.30, H 5.71; found C 47.14, H 5.61.

12-[3-(4-Hydroxymethyl-2-methoxyphenoxy)propoxy]-3,8,13-trimethoxy-10,15-dihydro-5*H*-tribenzo[*a*,*d*,*g*]cyclononene-2,7-diol (18). General Procedure A: Compound **13** (0.63 g, 1.96 mmol) was added in one portion to a stirred solution of **6** (0.8 g, 1.96 mmol) and cesium carbonate (1.28 g, 3.93 mmol) in dry DMF (35 mL). The mixture was stirred overnight at 80 °C under an argon atmosphere. After cooling to room temperature, the mixture was poured into water and the product extracted with ethyl acetate. The combined organic layers were washed several times with brine and then dried over Na_2SO_4. The solvent was removed to leave a residue which was chromatographed on silica gel (eluent: EtOAc). The second spot detected by TLC was collected and corresponds to the expected derivative **18** (0.38 g, 32%) which was isolated as a glassy solid. ^1H NMR (500 MHz, $CDCl_3$, 20 °C): δ = 6.91−6.73 (m, 9 H, Ar), 5.40 (s, 1 H, OH), 5.37 (s, 1 H, OH), 4.715 (d, ^2J = 14.0 Hz, 2 H, CH_a), 4.70 (d, ^2J = 13.5 Hz, 2 H, CH_a), 4.69 (d, ^2J = 13.5 Hz, 2 H, CH_a), 4.57 (d, ^3J = 6.0 Hz, 2 H, CH_2), 4.28−4.18 (m, 2 H, OCH_2), 4.16 (t, ^3J = 6.5 Hz, 2 H, OCH_2), 3.84 (s, 3 H, OCH_3), 3.78 (s, 3 H, OCH_3), 3.74 (s, 3 H, OCH_3), 3.72 (s, 3 H, OCH_3), 3.49 (d, ^2J = 13.5 Hz, 6 H, CH_e), 2.27 (quint, ^3J = 6.5 Hz, 2 H, CH_2), 1.61 (t, ^3J = 6.0 Hz, 1 H, OH) ppm. ^{13}C NMR (125.67 MHz,

$CDCl_3$, 20 °C): δ = 149.48, 148.17, 147.80, 146.76, 145.21, 145.17, 144.05, 143.98, 133.81, 132.47, 132.28, 132.17, 131.82, 131.31, 131.15, 119.40, 115.50 (2 C), 115.30, 113.52, 113.10, 112.18, 112.13, 110.77, 65.93, 65.71, 65.23, 56.06 (1 C, O*C*H_3), 56.01 (1 C, O*C*H_3), 55.88 (1 C, O*C*H_3), 55.67 (1 C, O*C*H_3), 36.35 (1 C, *C*$H_{a,e}$), 36.19 (2 C, *C*$H_{a,e}$), 29.05 (1 C, *C*H_2) ppm. HRMS (LSIMS): exact mass calcd. for $C_{35}H_{37}O_9$ $[M - H]^-$ 601.2438, found 601.2432.

12-[3-(4-Hydroxymethyl-2-methoxyphenoxy)butoxy]-3,8,13-trimethoxy-10,15-dihydro-5*H*-tribenzo[*a*,*d*,*g*]cyclononene-2,7-diol (19): Using general procedure A, **19** (0.4 g, 33%) was obtained from cyclotriveratrylene **6** (0.8 g, 1.96 mmol), compound **14** (0.65 g, 1.93 mmol) and cesium carbonate (1.28 g, 3.92 mmol) in DMF (45 mL). ^{1}H NMR (500 MHz, $CDCl_3$, 20 °C): δ = 6.87−6.74 (m, 9 H, Ar), 5.45 (s, 1 H, OH), 5.40 (s, 1 H, OH), 4.72 (d, ^2J = 13.5 Hz, 1 H, CH_a), 4.70 (d, ^2J = 13.5 Hz, 1 H, CH_a), 4.69 (d, ^2J = 13.5 Hz, 1 H, CH_a), 4.59 (d, ^3J = 6.0 Hz, 2 H, CH_2), 4.10−3.96 (m, 4 H, OCH_2), 3.84 (s, 3 H, OCH_3), 3.79 (s, 3 H, OCH_3), 3.73 (s, 3 H, OCH_3), 3.64 (s, 3 H, OCH_3), 3.48 (d, ^2J = 13.5 Hz, 3 H, CH_e), 1.98 (m, 4 H, CH_2), 1.61 (t, ^3J = 6.0 Hz, 1 H, OH) ppm. ^{13}C NMR (125.67 MHz, $CDCl_3$, 20 °C): δ = 149.49, 148.25, 147.96, 146.94, 145.22, 145.17, 144.08 (2 C), 133.57, 132.56, 132.33, 132.07, 131.66, 131.28, 131.12, 119.41, 115.59, 115.50, 115.06, 113.53, 112.79, 112.18, 112.08, 110.82, 68.80, 68.61, 65.36, 56.10 (1 C, O*C*H_3), 56.06 (1 C, O*C*H_3), 55.91 (1 C, O*C*H_3), 55.63 (1 C, O*C*H_3), 36.44 (1 C, *C*$H_{a,e}$), 36.21 (2 C, *C*$H_{a,e}$), 25.98 (1 C, *C*H_2), 25.90 (1 C, *C*H_2) ppm. HRMS (LSIMS): exact mass calcd. for $C_{36}H_{39}O_9$ $[M - H]^-$ 615.2594, found 615.2595.

{3-Methoxy-4-[3-(3,8,13-trimethoxy-7,12-bis{2-[2-methoxy-4-(tetrahydropyran-2-yloxymethyl)phenoxy]ethoxy}-10,15-dihydro-5*H*-tribenzo[*a*,*d*,*g*]cyclononen-2-yloxy)propoxy]phenyl}methanol (21): Using general procedure A, compound **21** (0.5 g, 72%) was obtained from **18** (0.37 g, 0.62 mmol), **15** (0.58 g, 1.48 mmol) and cesium carbonate (0.81 g, 2.48 mmol) in DMF (20 mL). ^{1}H NMR (500 MHz, $CDCl_3$, 20 °C): δ = 7.01−6.78 (m, 15 H, Ar), 4.72 (d, ^2J = 13.0 Hz, 3 H, CH_a), 4.70 (d, ^2J = 11.5 Hz, 2 H), 4.66 (m, 2 H), 4.57 (d, ^3J = 6.0 Hz, 2 H, C*H*$_2$OH), 4.42 (d, ^2J = 11.5 Hz, 2 H), 4.33 (m, 8 H, CH_2), 4.26−4.16 (m, 2 H, OCH_2), 4.15 (t, ^3J = 6.0 Hz, 2 H, OCH_2), 3.90 (m, 2 H), 3.84 (s, 6 H, 2 × OCH_3), 3.77 (s, 3 H, OCH_3), 3.72 (s, 3 H, OCH_3), 3.69 (s, 6 H, 2 × OCH_3), 3.56−3.48 (m, 5 H), 2.27 (p, ^3J = 6.0 Hz, 2 H, CH_2), 1.90−1.50 (m, 13 H, THP + OH) ppm. ^{13}C NMR (125.67 MHz, $CDCl_3$, 20 °C): δ = 149.48, 149.43 (2 C), 148.42, 148.37, 148.21, 147.74, 147.50 (2 C), 146.85, 146.77, 146.76, 133.94, 133.00, 132.91, 132.12, 131.90, 131.80, 131.66, 131.53 (2 C), 120.52 (2 C), 119.34, 116.51, 116.44, 115.20, 113.74, 113.70, 113.48 (3 C), 113.03, 111.84 (2 C), 110.73, 97.56 (2 C), 68.69 (2 C), 68.10 (2 C), 67.59 (2 C), 65.85, 65.65, 65.20, 62.28 (2 C), 56.16 (1 C, O*C*H_3), 56.08 (1 C, O*C*H_3), 56.04 (1 C, O*C*H_3), 55.81 (2 C, 2 × O*C*H_3), 55.64 (1 C, O*C*H_3), 36.36 (3 C), 30.56 (2 C), 29.09 (1 C, *C*H_2), 25.41 (2 C), 19.44 (2 C) ppm. HRMS (LSIMS): exact mass calcd. for $C_{65}H_{78}O_{17}$ $[M]^+$ 1130.5239, found 1130.5286.

{3-Methoxy-4-[2-(3,8,13-trimethoxy-7,12-bis{3-[2-methoxy-4-(tetrahydropyran-2-yloxymethyl)phenoxy]propoxy}-10,15-dihydro-5*H*-tribenzo[*a*,*d*,*g*]cyclononen-2-yloxy)ethoxy]phenyl}methanol (20): Using general procedure A, compound **20** (0.75 g, 74%) was obtained from **17** (0.52 g, 0.88 mmol), **16** (0.86 g, 2.12 mmol) and cesium carbonate (1.15 g, 3.5 mmol) in DMF (30 mL). ^{1}H NMR (500 MHz, $CDCl_3$, 20 °C): δ = 6.98−6.77 (m, 15 H, Ar), 4.71 (d, ^2J = 13.5 Hz, 3 H, CH_a), 4.69 (d, ^2J = 11.5 Hz, 2 H), 4.65 (m, 2 H), 4.58 (d, ^3J = 6.0 Hz, 2 H, CH_2OH), 4.40 (d, ^2J = 11.5 Hz, 2 H), 4.38−4.29 (m, 4 H, OCH_2), 4.26−4.12 (m, 8 H, OCH_2), 3.90 (m, 2 H), 3.82 (s, 6 H, 2 × OCH_3), 3.73 (s, 3 H, OCH_3), 3.725 (s, 3 H, OCH_3), 3.72 (s, 3 H, OCH_3), 3.65 (s, 3 H, OCH_3), 3.58−3.46 (m, 5 H), 2.28 (m, 4 H, CH_2), 1.90−1.50 (m, 13 H, THP+OH) ppm. ^{13}C NMR (125.67 MHz, $CDCl_3$, 20 °C): δ = 149.66, 149.32 (2 C), 148.46, 148.15, 148.09, 147.77 (2 C), 147.42, 146.85 (2 C), 146.73, 134.52, 133.05, 132.12, 132.10, 131.84, 131.83, 131.71, 130.99, 130.97, 120.53 (2 C), 119.30, 116.70 (2 C), 115.10, 113.81, 113.71 113.53 (2 C), 112.89 (2 C), 111.72 (2 C), 110.88, 97.49 (2 C), 68.71 (2 C), 68.09 (2 C), 67.75 (2 C), 65.87, 65.59, 65.14, 62.26 (2 C), 56.05 (3 C, 3 × O*C*H_3), 55.80 (2 C, 2 × O*C*H_3), 55.69 (1 C, O*C*H_3), 36.36 (3 C, *C*$H_{a,e}$), 30.56 (2 C), 29.07 (2 C, *C*H_2), 25.42 (2 C), 19.44 (2 C) ppm. HRMS (LSIMS): exact mass calcd. for $C_{66}H_{80}NaO_{17}$ $[M + Na]^+$ 1167.5293, found 1167.5289.

{3-Methoxy-4-[4-(3,8,13-trimethoxy-7,12-bis{2-[2-methoxy-4-(tetrahydropyran-2-yloxymethyl)phenoxy]ethoxy}-10,15-dihydro-5*H*-tribenzo[*a*,*d*,*g*]cyclononen-2-yloxy)butoxy]phenyl}methanol (22): Using general procedure A, compound **22** (0.59 g, 79%) was obtained from **19** (0.40 g, 0.65 mmol), **15** (0.61 g, 1.50 mmol) and cesium carbonate (0.85 g, 2.6 mmol) in DMF (25 mL). ^{1}H NMR (500 MHz, $CDCl_3$, 20 °C): δ = 7.01−6.78 (m, 15 H, Ar), 4.72 (d, ^2J = 13.5 Hz, 3 H, CH_a), 4.70 (d, ^2J = 11.5 Hz, 2 H), 4.66 (m, 2 H), 4.58 (d, ^3J = 6.0 Hz, 2 H, CH_2OH), 4.42 (d, ^2J = 11.5 Hz, 2 H), 4.34 (m, 8 H, CH_2), 4.10−3.96 (m, 4 H, CH_2), 3.90 (m, 2 H), 3.84 (s, 6 H, 2 × OCH_3), 3.72 (s, 3 H, OCH_3), 3.70 (s, 9 H, 3 × OCH_3), 3.56−3.48 (m, 5 H), 1.98 (m, 4 H, CH_2), 1.90−1.50 (m, 13 H, THP+OH) ppm. ^{13} C NMR (125.67 MHz, $CDCl_3$, 20 °C): δ = 149.42 (2 C), 149.39, 148.40, 148.30, 148.22, 147.82, 147.49 (2 C), 147.00, 146.78 (2 C), 133.76, 132.96, 132.84, 131.99, 131.91, 131.88, 131.53, 131.51, 131.49, 120.49 (2 C), 119.31, 116.53, 116.50, 114.96, 113.73, 113.53 (3 C), 113.47, 112.78, 111.85 (2 C), 110.72, 97.54 (2 C), 68.66 (3 C), 68.54, 68.12 (2 C), 67.59 (2 C), 65.18, 62.24 (2 C), 56.16 (1 C, O*C*H_3), 56.08 (1 C, O*C*H_3), 56.04 (1 C, O*C*H_3), 55.81 (2 C, 2 × O*C*H_3), 55.64 (1 C, O*C*H_3), 36.40 (1 C, *C*$H_{a,e}$), 36.33 (2 C, *C*$H_{a,e}$), 30.53 (2 C), 25.93 (1 C, *C*H_2), 25.83 (1 C, *C*H_2), 25.38 (2 C), 19.42 (2 C) ppm. HRMS (LSIMS): exact mass calcd. for $C_{66}H_{80}O_{17}$ $[M]^+$ 1144.5396, found 1144.5375.

Cryptophane-223 (1). General Procedure B: In a 1-L rotary evaporator flask, compound **21** (0.6 g, 0.53 mmol) was dissolved in chloroform (6 mL). Then formic acid (600 mL) was added in one portion and the solution was heated at 55 °C for 2 h 30 min with slow rotation. The solvent was evaporated under reduced pressure and chloroform was added to remove residual formic acid by azeotropic distillation. The cryptophane was purified by column chromatography on silica gel (CH_2Cl_2/acetone, 90:10) and washed with a few milliliters of diethyl ether on a frit. A second run of column chromatography (CH_2Cl_2/acetone, 90:10) yielded pure cryptophane-223 (0.17 g, 35%); decomp. above 300 °C. ^{1}H NMR (500 MHz, $CDCl_3$, 20 °C): δ = 6.77 (s, 2 H, Ar), 6.73 (s, 2 H, Ar), 6.67 (s, 2 H, Ar), 6.66 (s, 2 H, Ar), 6.64 (s, 2 H, Ar), 6.55 (s, 2 H, Ar), 4.61 (d, ^2J = 14.0 Hz, 4 H, CH_a), 4.59 (d, ^2J = 14.0 Hz, 2 H, CH_a), 4.31−4.22 (m, 2 H, OCH_2), 4.16−3.98 (m, 8 H, OCH_2), 3.89−3.82 (m, 2 H, OCH_2), 3.81 (s, 6 H, 2 × OCH_3), 3.79 (s, 6 H, 2 × OCH_3), 3.77 (s, 6 H, 2 × OCH_3), 3.41 (d, ^2J = 14.0 Hz, 2 H, CH_e), 3.39 (d, ^2J = 14.0 Hz, 4 H, CH_e), 2.29 (m, 2 H, CH_2) ppm. ^{13}C NMR (125.67 MHz, $CDCl_3$, 20 °C): δ = 149.45 (2 C), 149.37 (2 C), 147.44 (2 C), 147.31 (2 C), 146.68 (2 C), 146.52 (2 C), 133.97 (2 C), 133.83 (2 C), 132.43 (2 C), 131.39 (2 C), 131.25 (2 C), 130.48 (2 C), 120.43 (2 C), 120.33 (2 C), 114.01 (2 C), 113.46 (2 C), 112.21 (2 C), 112.08 (2 C), 69.63 (2 C), 68.94 (2 C), 63.66 (2 C), 56.22 (2 C, 2 × O*C*H_3), 55.54 (2 C, 2 × O*C*H_3), 55.43 (2 C, 2 × O*C*H_3), 36.41 (2 C, *C*$H_{a,e}$), 36.05 (2 C, *C*$H_{a,e}$), 35.99 (2 C, *C*$H_{a,e}$), 29.84 (1 C, *C*H_2) ppm. HRMS (LSIMS): exact mass calcd. for $C_{55}H_{56}O_{12}$ $[M]^+$, 908.377, found 908.3780.

Cryptophane-233 (2): Using general procedure B, cryptophane-233 (0.18 g, 37%) was obtained from compound **20** (0.6 g, 0.52 mmol) in formic acid (600 mL); decomp. above 300 °C. ^{1}H NMR (500 MHz, $CDCl_3$, 20 °C): δ = 6.74 (s, 2 H, Ar), 6.68 (s, 2 H, Ar), 6.66 (s, 2 H, Ar), 6.64 (s, 2 H, Ar), 6.59 (s, 2 H, Ar), 6.57 (s, 2 H, Ar), 4.62 (d, ^2J = 14.0 Hz, 6 H, CH_a), 4.20−4.10 (m, 2 H), 4.10−3.96 (m, 6 H), 3.87 (m, 4 H), 3.82 (s, 6 H, 2 × OCH_3), 3.81 (s, 6 H, 2 × OCH_3), 3.77 (s, 6 H, 2 × OCH_3), 3.41 (d, ^2J = 14.0 Hz, 4 H, CH_e), 3.38 (d, ^2J = 13.5 Hz, 2 H, CH_e), 2.29 (m, 4 H, CH_2) ppm. ^{13}C NMR (125.67 MHz, $CDCl_3$, 20 °C): δ = 149.22 (2 C), 147.28 (2 C), 147.23 (2 C), 147.20 (2 C), 147.05 (2 C), 146.53 (2 C), 133.71 (2 C), 132.05 (2 C), 131.12 (2 C), 131.05 (2 C), 130.91 (2 C), 130.61 (2 C), 120.26 (2 C), 113.38 (2 C), 112.29 (2 C), 112.19 (2 C), 112.15 (2 C), 112.03 (2 C), 69.42 (2 C), 63.72 (2 C), 63.51 (2 C), 55.82 (2 C, 2 × O*C*H_3), 55.74 (2 C, 2 × O*C*H_3), 55.37 (2 C, 2 × O*C*H_3), 36.26 (2 C, *C*$H_{a,e}$), 36.14 (2 C, *C*$H_{a,e}$), 35.85 (2 C, *C*$H_{a,e}$), 29.68 (2 C, *C*H_2) ppm. HRMS (LSIMS): exact mass calcd. for $C_{56}H_{58}O_{12}$ $[M]^+$ 922.3928, found 922.3990.

Cryptophane-224 (3): Using general procedure B, cryptophane-224 (0.22 g, 38%) was obtained from compound **22** (0.58 g, 0.51 mmol) in formic acid (600 mL); decomp. above 300 °C. ^{1}H NMR (500 MHz, $CDCl_3$, 20 °C): δ = 6.81 (s, 2 H, Ar), 6.72 (s, 2 H, Ar), 6.69 (s, 2 H, Ar), 6.65 (s, 2 H, Ar), 6.63 (s, 2 H, Ar), 4.61 (d, ^2J = 14.0 Hz, 4 H, CH_a), 4.56 (d, ^2J = 14.0 Hz, 2 H, CH_a), 4.38−4.30 (m, 2 H, OCH_2), 4.25−4.18 (m, 2 H, OCH_2), 4.15−4.10 (m, 2 H, OCH_2), 4.07−3.93 (m, 4 H, OCH_2), 3.91−3.83 (m, 2 H, OCH_2), 3.83 (s, 6 H, 2 × OCH_3), 3.75 (s, 6 H, 2 × OCH_3), 3.70 (s, 6 H, 2 × OCH_3), 3.40 (d, ^2J = 14.0 Hz, 6 H, CH_e), 1.81 (m, 4 H, CH_2) ppm. ^{13}C NMR (125.67 MHz, $CDCl_3$, 20 °C): δ = 149.42 (2 C), 148.88 (2 C), 148.55 (2 C), 146.63 (2 C), 146.41 (2 C), 146.25 (2 C), 134.24 (2 C), 133.53 (2 C), 132.16 (4 C), 131.54 (2 C), 131.08 (2 C), 120.16 (2 C), 119.00 (2 C), 117.05 (2 C), 114.80 (2 C), 113.02 (2 C), 112.79 (2 C), 69.65 (2 C), 68.62 (2 C), 68.07 (2 C), 56.71 (2 C, 2 × O*C*H_3), 55.39 (2 C, 2 × O*C*H_3), 55.14 (2 C, 2 × O*C*H_3), 36.19 (2 C, *C*$H_{a,e}$), 36.11 (4 C, *C*$H_{a,e}$), 24.76 (2 C, 2 × *C*H_2) ppm. HRMS (LSIMS): exact mass calcd. for $C_{56}H_{58}O_{12}$ $[M]^+$ 922.3928, found 922.3926.

Acknowledgments

We thank Prof. D. M. Rudkevich and co-workers for providing us with the calculations of the inner space volumes of the cryptophanes.

[1] D. J. Cram, M. E. Tanner, C. B. Knobler, *J. Am. Chem. Soc.* **1991**, *113*, 7717−7727.
[2] T. A. Robbins, C. B. Knobler, D. R. Bellew, D. J. Cram, *J. Am. Chem. Soc.* **1994**, *116*, 111−122.
[3] N. Branda, R. M. Grotzfeld, C. Valdés, J. Rebek, Jr., *J. Am. Chem. Soc.* **1995**, *117*, 85−88.
[4] C. Valdés, U. P. Spiz, L. M. Toledo, S. W. Kubik, J. Rebek, Jr., *J. Am. Chem. Soc.* **1995**, *117*, 12733−12745.
[5] K. Bartik, M. Luhmer, J.-P. Dutasta, A. Collet, J. Reisse, *J. Am. Chem. Soc.* **1998**, *120*, 784−791.
[6] T. Brotin, A. Lesage, L. Emsley, A. Collet, *J. Am. Chem. Soc.* **2000**, *122*, 1171−1174.
[7] K. Bartik, M. Luhmer, J. Reisse, A. Collet, J.-P. Dutasta, unpublished results.
[8] S. Mecozzi, J. Rebek, Jr., *Chem. Eur. J.* **1998**, *4*, 1016−1022.
[9] T. Brotin, T. Devic, A. Lesage, L. Emsley, A. Collet, *Chem. Eur. J.* **2001**, *7*, 1561−1573.
[10] T. Brotin, M. Darzac, D. Forest, M. Becchi, J.-P. Dutasta, *J. Mass Spectrom.* **2001**, *36*, 1092−1097.
[11] I. Gosse, J.-P. Dutasta, M. Perrin, A. Thozet, *New J. Chem.* **1999**, *23*, 545−548.
[12] J. Canceill, A. Collet, G. Gottarelli, P. Palmieri, *J. Am. Chem. Soc.* **1987**, *109*, 6454−6464.
[13] J. Canceill, L. Lacombe, A. Collet, *J. Am. Chem. Soc.* **1985**, *107*, 6993−6996.
[14] A. Tambuté, J. Canceill, A. Collet, *Bull. Chem. Soc. Jpn.* **1989**, *62*, 1390−1392.
[15] S. Akabori, M. Miura, M. Takeda, S. Yuzawa, Y. Habata, T. Ishii, *Supramol. Chem.* **1996**, *7*, 187−193.
[16] The rapid loss of efficiency of the Chiralpak OT^+ column did not allow us to perform a correct analysis of compound **3**.
[17] J. Ripmeester, *J. Am. Chem. Soc.* **1982**, *104*, 289−290.
[18] Kindly provided by Prof. Rudkevich and co-workers. Cryptophanes were first minimized with Macromodel 7.1, Amber force field, then the program GRASP was used to estimate the volume of the internal cavities of cryptophanes as described in ref.[8].
[19] M. M. Spence, S. M. Rubin, I. E. Dimitrov, E. J. Ruiz, D. E. Wemmer, A. Pines, S. Q. Yao, F. Tian, P. G. Shultz, *Proc. Natl. Acad. Sci. USA* **2001**, *98*, 10654−10657.
[20] M. Pons, O. Millet, *Prog. Nucl. Magn. Reson. Spectrosc.* **2001**, *38*, 267−324.
[21] The matrix **L** may be calculated numerically by solving the following system: $R = (\ln A_{ij})/\tau_m$, where $A_{ij} = I_{ij}(\tau_m)/M^0_j$ is the experimental matrix that contains all the intensities for each site and for the three selective irradiations.
[22] M. Darzac, T. Brotin, D. Bouchu, J.-P. Dutasta, *Chem. Commun.* **2002**, 48−49.

Received September 6, 2002
[O02500]